http://ansinet.com/itj

ITJ

ISSN 1812-5638

INFORMATION TECHNOLOGY JOURNAL

ANSInet
Asian Network for Scientific Information
308 Lasani Town, Sargodha Road, Faisalabad - Pakistan

Information Technology Journal 9 (3): 583-588, 2010
ISSN 1812-5638

Asymmetric Combined Cycle-Encoding Light 3D Measurement Technique

S. Li-Na, Y. Xiao-Yang and F. Xiao
The Higher Educational Key Laboratory for Measuring and Control Technology and Instrumentations, Harbin University of Science and Technology, Heilongjiang Province, People's Republic of China

Abstract: In order to eliminate the periodic dislocation and improve the measurement speed, a method named asymmetric combined cycle-encoding is presented. This method replaces the sinusoidal phase-shifting with trapezoidal for optimizing measurement speed. The traditional periodic dislocation is solved by building the non-symmetrical correspondence between two kinds of codes. The inherent error of cyclic code is eliminated by modify the period of cyclic code and trapezoidal phase shifting intensity code. The measurement speed is improved significantly. Experimental results show that the presented method in this study greatly reduces the measurement error. The measurement error is less than 1.7 mm in the range of 1000 mm.

Key words: Asymmetric, cycle-encoding, 3D measurement, machine vision

INTRODUCTION

Structured light encoding is the most promising direction of development in the structured light 3D measurement technology (Sang, 2001; Guan *et al.*, 2007). And it is widely used in areas such as machine vision. It can't only ensure the efficiency of measurement, but also simplify identification. This technology influences the measurement accuracy, speed and reliability, which plays an important role in the structured light method for data acquisition. Therefore, it is great significance to studying on the coding techniques in 3D measurement (Li *et al.*, 2006).

Structured light encoding techniques include time-encoding, spatial-encoding and direct-encoding. Combination of two or more high-quality encoding technology can integrate the advantages of a single code, improve the comprehensive indicators of the measurement, thus, it is a new trend on the structured light coding technology. In the existing technologies, the encoding method based on the cyclic code combined with phase-shifting (Gühring, 2001; Lee *et al.*, 2004; Pan *et al.*, 2004) such as symmetric combined cycle-encoding, can be sufficient to retain the advantages of cyclic codes. The system is economically viable, easy to compute and has a higher spatial resolution and accuracy (Pan *et al.*, 2003; Dong *et al.*, 2000). Because there are an inherent period error of the cyclic code (Yu and Wu, 2008) and period dislocation to affect measure speed and accuracy, they must be determined and adjusted. In this study, a method called asymmetric combined cycle-encoding is presented and it could effectively solve the above problems.

PRINCIPLE OF MEASUREMENT

System architecture: The basic structured light system is component by the projector and camera shown in Fig 1. The projector is commonly used to project cycle-encoding and trapezoidal phase-shifting patterns onto the object being measured in turn. The images of the object with the projected patterns are captured by camera. The modulated images captured by a camera are processed by a computer and then the 3D coordinates are obtained with triangulation (Davis *et al.*, 2005).

Principle of asymmetric combined cycle-encoding light: Asymmetric combined cycle-encoding is composed by the cyclic code and trapezoidal phase-shifting

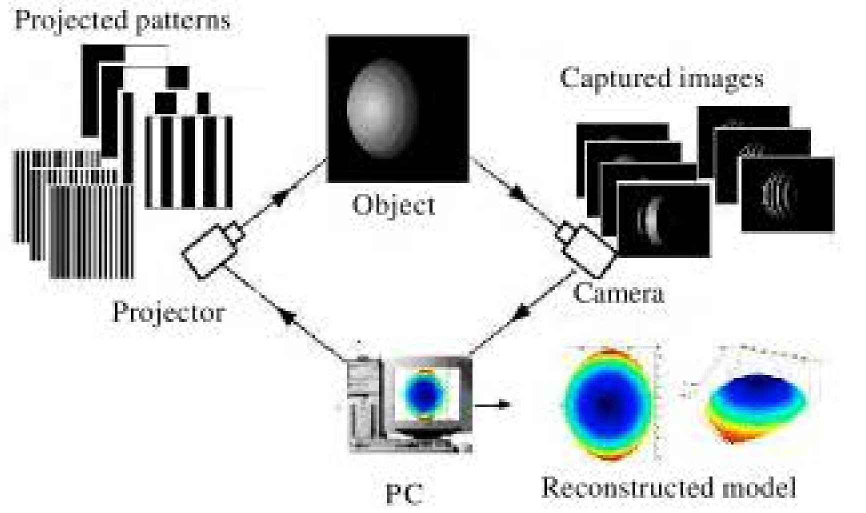

Fig. 1: The basic structured light system

Corresponding Author: Shan Li-Na, P.O. Box 326, No. 4 Lin Yuan Road, Xiang Fang District, Harbin University of Science and Technology, Harbin City, Heilongjiang Province, 150040, People's Republic of China Tel/Fax: 86-0451-86392305

intensity code. In this study, four cyclic code patterns and three-step trapezoidal phase- shifting patterns are used to project.

First of all, four cyclic code stripes are projected onto the measured object from the projector. The projector angle is roughly divided into 16 regions. Every region has a cyclic code period k. Secondly, the measured object is projected three strength yards pattern. The intensity of three modulated images is determined to obtain intensity code period. We calculate the strength values to get the intensity ratio and then obtain absolute strength ratio in accordance with strength ratio and recycling yards cycle. The absolute strength ratio is mapped to the projection angle of sampling points, which to achieve to divide accurately projection angle space.

A trapezoidal phase-shift intensity code (Zhang, 2003) changed according to the phase-shift fringe patterns in the trapezoidal period and it included a positive and a negative trapezoidal. This study adopts three-step approach that 1/3 trapezoidal phase-shift period marked as T was shifted twice in the vertical position of the projection patterns. Projection order is shown in Fig. 2, where, I_1, I_2, I_3 are the three cross sectional of projection patterns. Figure 3 shows the trapezoidal phase-shifting intensity code projection patterns.

Two kinds of coding period were reset for eliminating the inherent period error because of the cyclic code, that is 5/6 trapezoidal phase-shifting period is included in a cyclic code period (Xiaoyang *et al*., 2007)

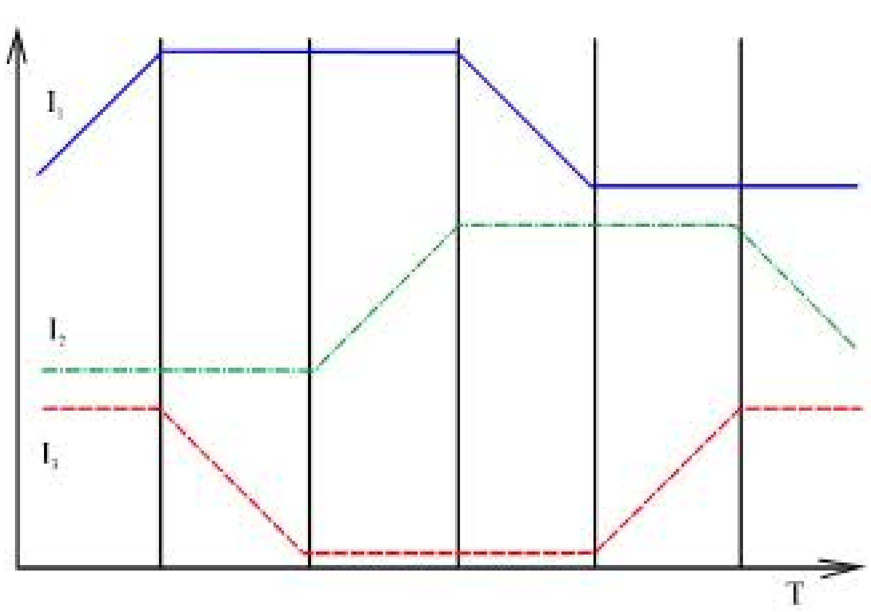

Fig. 2: Trapezoidal phase-shifting intensity code projection order

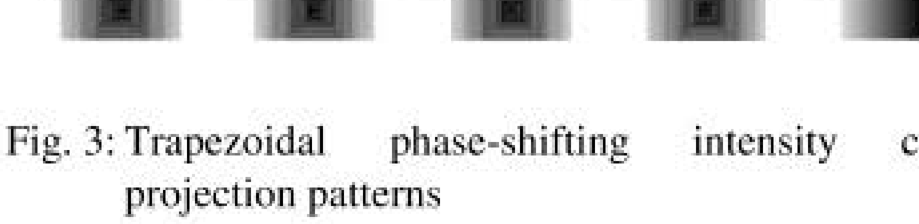

Fig. 3: Trapezoidal phase-shifting intensity code projection patterns

instead of a whole trapezoidal phase-shifting period. Trapezoidal slope center corresponds to the trip point of the smallest cyclic code is the relationship between the smallest cyclic code period and trapezoidal phase-shifting intensity code, shown in Fig 4. The smallest cyclic code period is equal to 20 pixels.

Calculating intensity ratio is the key of asymmetric combined cycle-encoding. The ratio combined with the cyclic code period to get the linear absolute intensity ratio, which is corresponded to the projection angle. Then the coordinates of measured object can be obtained by the use of triangulation. The intensity of every measured point is named I, which is the intensity projection of trapezoidal phase-shifting intensity code in Fig. 2.

The intensity of $I_{min}(x, y)$, $I_{med}(x, y)$, $I_{max}(x, y)$ are judged according to the pixel value, where, $I_{min}(x, y)$, $I_{med}(x, y)$, $I_{max}(x, y)$ are the intensities of the median, minimum and maximum intensity values at pixel (x, y), respectively. Then the intensity ratio of every point on the measured object can be obtained by applying the following Eq. 1.

$$r(x,y) = \frac{I_{med}(x,y) - I_{min}(x,y)}{I_{max}(x,y) - I_{min}(x,y)} \quad (1)$$

The intensity ratio, r(x, y), has a triangular shape whose value ranges from 0 to 1. A trapezoidal phase shifting period is shown in Fig. 5. To determine the

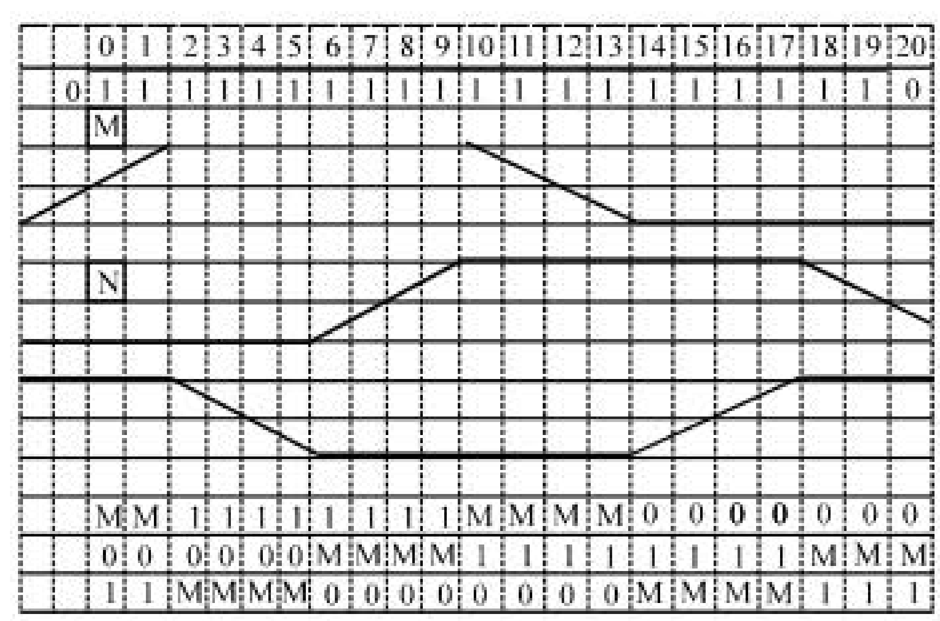

Fig. 4: The relationship between the first smallest cyclic code period and trapezoidal phase-shifting intensity code

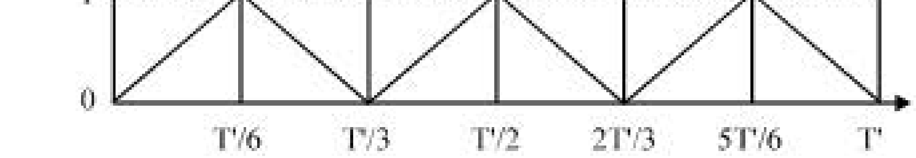

Fig. 5: The intensity ratios in a trapezoidal phase-shifting period

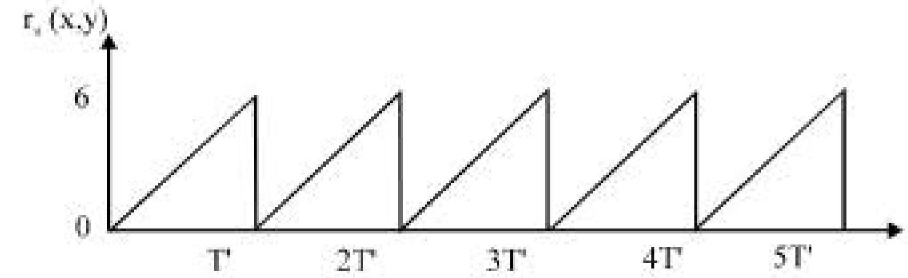

Fig. 6: Relative intensity ratios

intensity code period of pixel points, the intensity value of three trapezoidal phase-shifting patterns are arranged in the order and six samples are considered. These samples are taken at:

$$\begin{cases} I_2 < I_1 < I_3 & N=1 \\ I_2 < I_3 < I_1 & N=2 \\ I_3 < I_2 < I_1 & N=3 \\ I_3 < I_1 < I_2 & N=4 \\ I_1 < I_3 < I_2 & N=5 \\ I_1 < I_2 < I_3 & N=6 \end{cases} \tag{2}$$

where, N is the intensity code whose value ranges from 0 to 6. A trapezoidal phase-shifting period includes six intensity codes.

To obtain the linear correspondence between intensity ratios and the projection angle of sampling points by combining intensity code N with intensity ratio r, the relative intensity ratios are calculated as follows:

$$r_\phi = 2\times \mathrm{round}(\frac{N-1}{2}) + (-1)^{N+1}\frac{I_{med(x,y)} - I_{min(x,y)}}{I_{max(x,y)} - I_{min(x,y)}} \tag{3}$$

whose result is shown in Fig. 6. Then the absolute intensity ratios and the whole linear division of the measured space can be obtained by combining the cyclic code using the following equation:

$$\begin{cases} k=0,6,12 & r_\Psi = 6k + r_\Phi \\ k=1,7,13 & \begin{cases} N=6 & r_\Psi = 6(k-1)+r_\Phi \\ N<6 & r_\Psi = 6k + r_\Phi \end{cases} \\ k=2,8,14 & \begin{cases} N\geq 5 & r_\Psi = 6(k-1)+r_\Phi \\ N<5 & r_\Psi = 6k + r_\Phi \end{cases} \\ k=3,9,15 & \begin{cases} N\geq 4 & r_\Psi = 6(k-1)+r_\Phi \\ N<4 & r_\Psi = 6k + r_\Phi \end{cases} \\ k=4,10 & \begin{cases} N\geq 3 & r_\Psi = 6(k-1)+r_\Phi \\ N<3 & r_\Psi = 6k + r_\Phi \end{cases} \\ k=5,11 & \begin{cases} N\geq 3 & r_\Psi = 6(k-1)+r_\Phi \\ N<3 & r_\Psi = 6k + r_\Phi \end{cases} \end{cases} \tag{4}$$

The solving method for projection angles: Projection angles can be solved by applying the following equation:

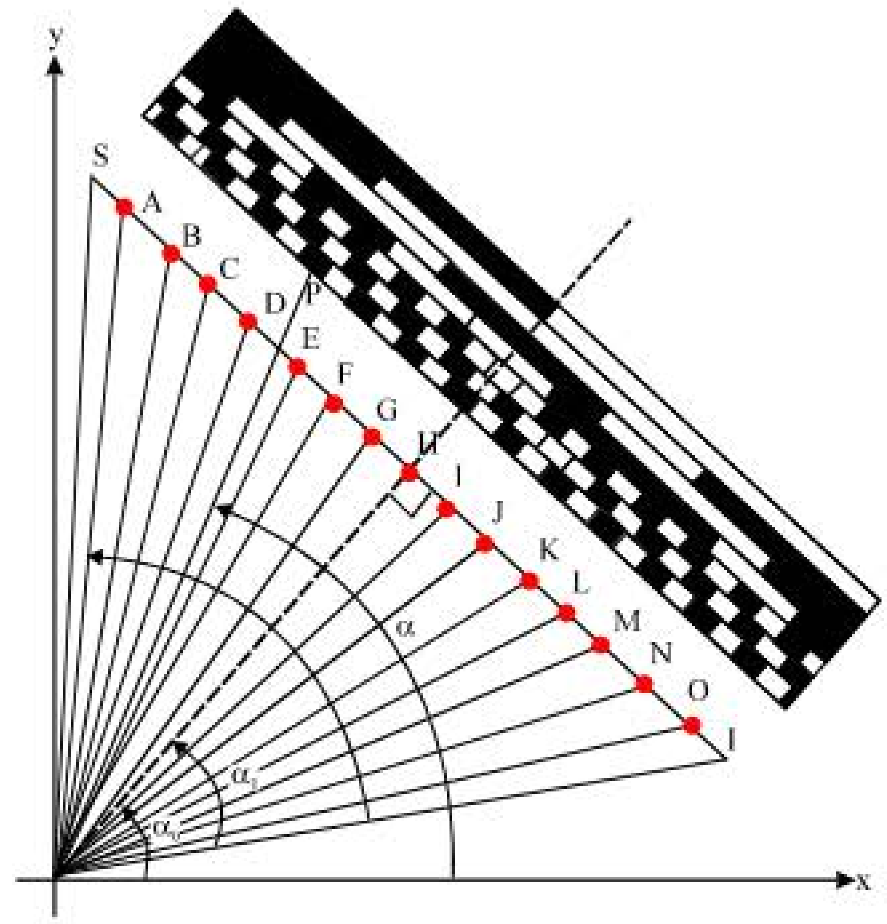

Fig. 7: The conversion relations between absolute intensity ratio and projector angle

$$\alpha = \alpha_0 + (1 - \frac{r_\Psi}{40})\alpha_1 \tag{5}$$

where, α_1 is a half of the whole projection angle; α_0 is the angle between the bisector of projection angle and X direction. It has a linear mapping of the absolute intensity ratios r_σ to the projection angle α in projection space which is shown in Fig. 7.

RESULTS

In this study, a projector, a video camera and measured objects are simulated by the 3D max composed the measurement system. The camera's field of view angle is 40° and its resolution is 1024×768. The projector's projection angle is 30°. MATLAB is used for image processing and reconstruction.

In the simulation, a plane on 549.495 mm was measured and reconstruction by the common combined cycle code and the asymmetric combined cycle-encoding. Figure 8a shows the reconstruction result that was used of the common combined cycle-encoding, the bump and the depression on the plane are period dislocations. Figure 8b was the result by asymmetric combined cycle-encoding and the plane is smooth, period dislocation is removed. Figure 9a is the error plane that was used of the combined cycle-encoding after correcting period dislocation, its error is less than 0.3 mm. But another error plane is shown in Fig. 9b which error is less than 0.05 mm. As the large errors generated by cyclic code are eliminated in this experiment.

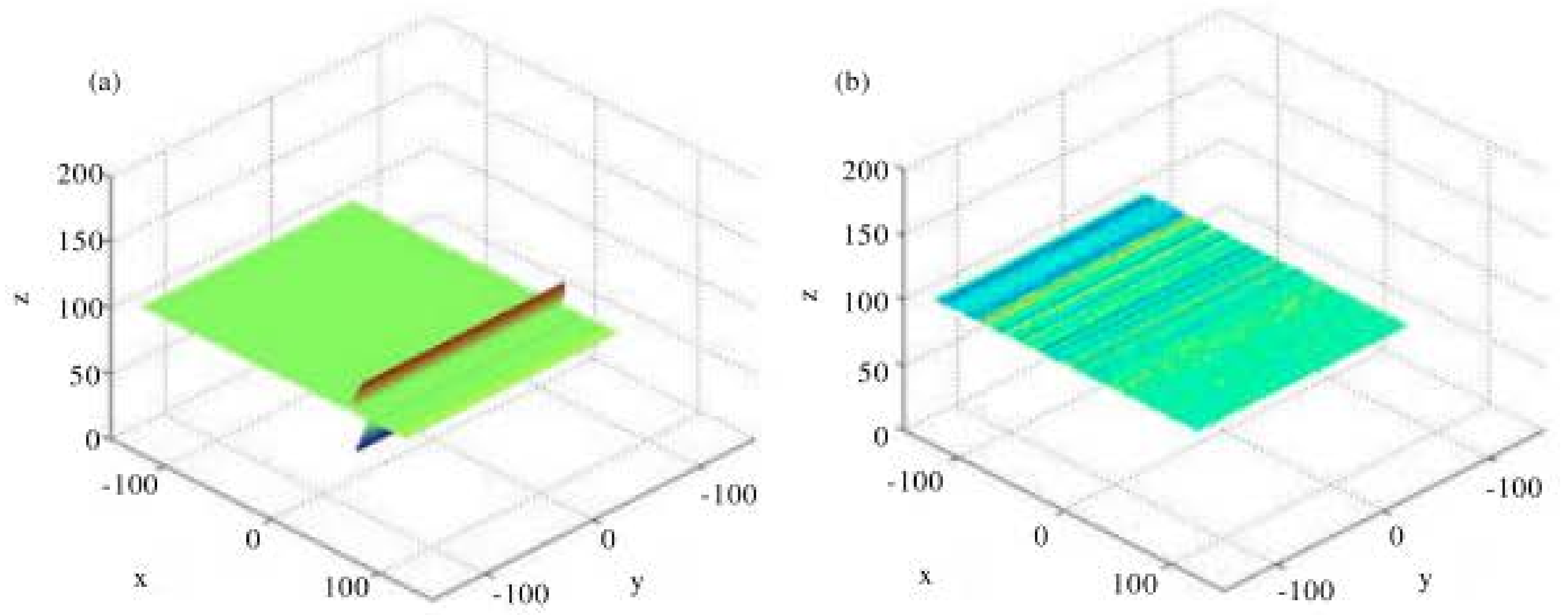

Fig. 8: (a, b) The plane of reconstruction experiment

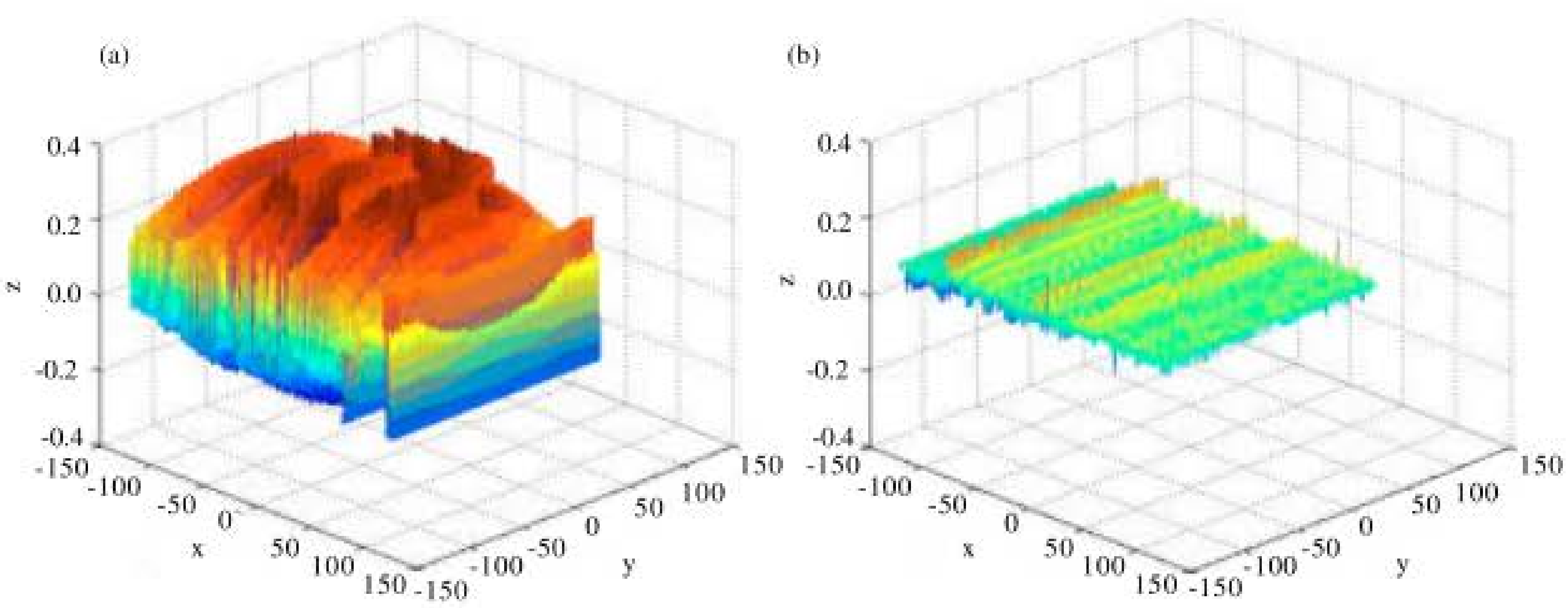

Fig. 9: (a, b) Maps of error plane

Another experiment measured many planes which depths were from 400 to 700 mm and reconstructed. To compare the measurement effects, four kinds of coding methods have been used. They are cyclic code I combined cycle-encoding II, combined cycle-coding with correcting period dislocation III and the asymmetric combined cycle-encoding IV. The results are shown in Table 1.

In practical experiment, the system consists of a computer, a digital light processing projector (MITSUBISHI XD300U), a 3CCD camera (HITACHI HV-F22) and a optical rail. To compare the measurement effects, four kinds of coding methods have also been used. The methods are same to the Table 1. They are shown in Table 2. In order to ensure more accurate results, the measurement data in Table 2 are the average of three measurements. Figure 10a is the reconstruction plane on 900 mm and its error map is shown in Fig. 10b. As it shows in Table 1, the measurement accuracy used asymmetric combined cycle-encoding is slightly better than the one used traditional combined cycle-encoding. This shows that the asymmetric combined cycle-encoding method ensures and improves the measurement accuracy at the same time speeding up the measurement.

Table 1: Results of simulation

Theory value (mm)	Method	Average value of measured (mm)	Average deviation (mm)	Variance (mm^2)	Measurement error (mm)
400	I	399.9968	0.3288	0.1451	0.7097
	II	399.8922	0.2718	5.5661	2.7229
	III	399.9998	0.0064	2.38×10^{-4}	0.0218
	IV	400.0001	0.0061	1.42×10^{-4}	0.0180
500	I	500.0041	0.4895	0.3213	1.0563
	II	499.9404	0.4088	9.0555	3.4180
	III	499.9998	0.0084	2.61×10^{-4}	0.0246
	IV	500.0002	0.0081	2.42×10^{-4}	0.0237
600	I	600.0058	0.7092	0.6697	1.5276
	II	599.9291	0.4789	15.1808	4.3752
	III	600.0003	0.0126	4.65×10^{-4}	0.0342
	IV	600.0002	0.0122	3.34×10^{-4}	0.0305
700	I	699.9817	0.9364	1.1805	2.0229
	II	699.8300	0.7590	31.4307	6.3653
	III	700.0006	0.0159	5.67×10^{-4}	0.0397
	IV	699.9997	0.0155	4.47×10^{-4}	0.0366

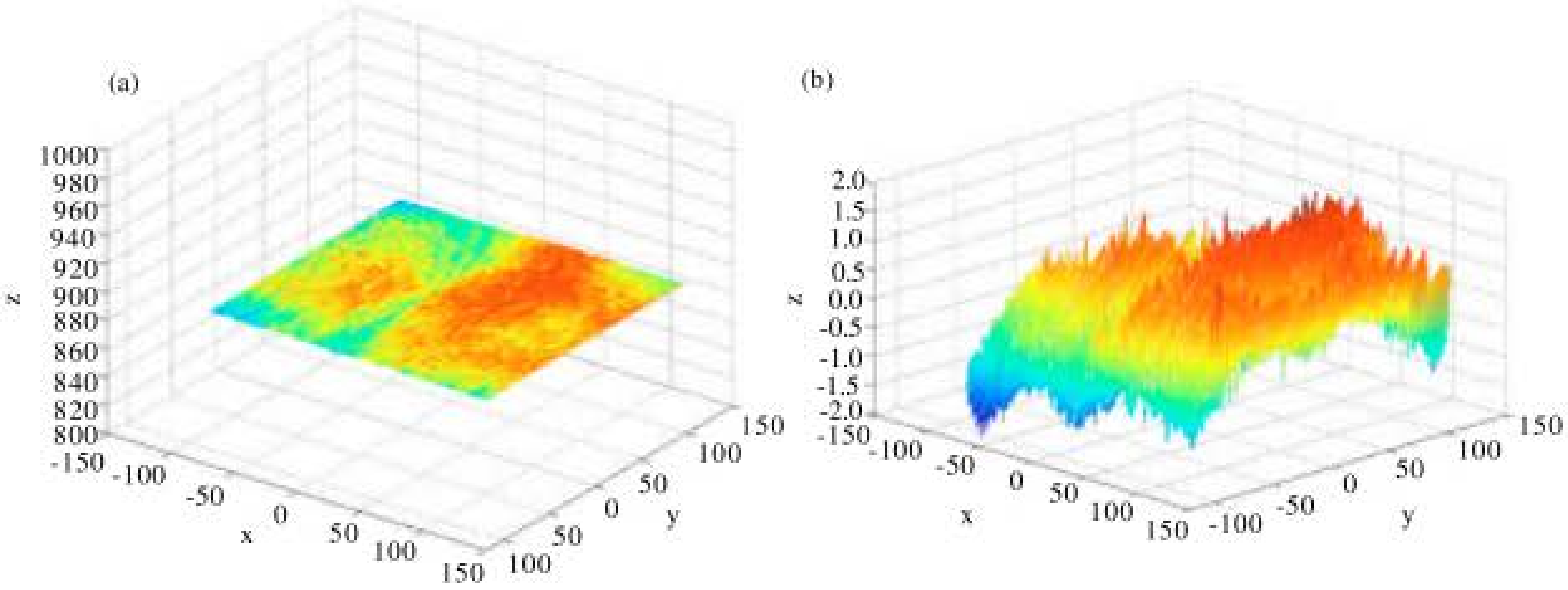

Fig. 10: Reconstruction plane on 900mm and its error map, (a) result of measurement (b) error map

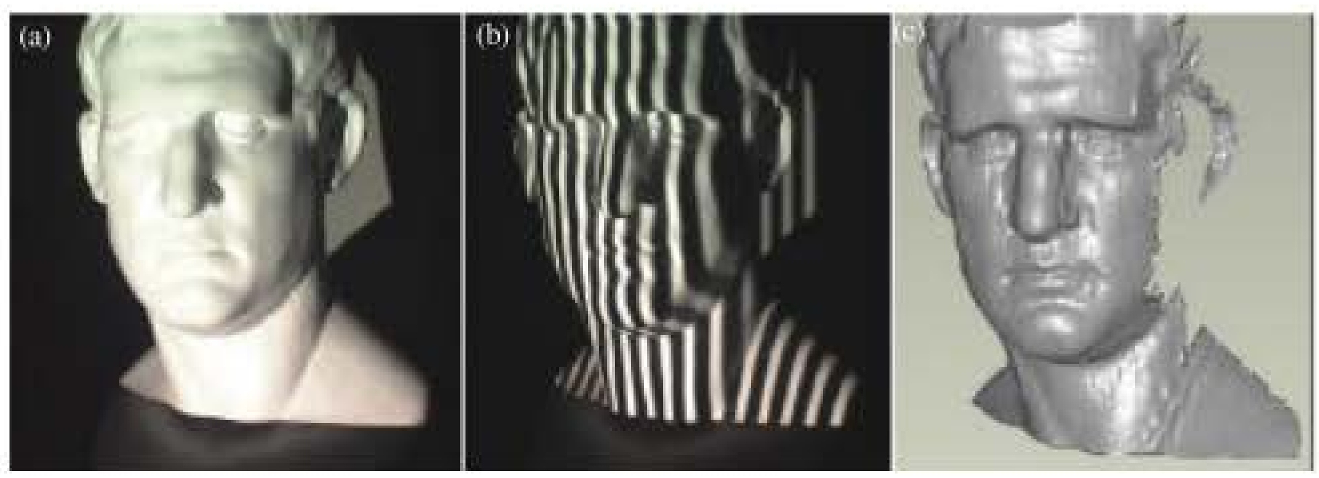

Fig. 11: Measurement experiment of the complex surface object, (a) measured object (b) measured object after projection (c) result of reconstruction

Table 2: Results of measurement

Theory value (mm)	Method	Average value of measured (mm)	Average deviation (mm)	Variance (mm^2)	Measurement error (mm)
700	I	700.1280	1.0385	1.2287	2.1470
	II	701.9515	1.7453	24.5639	6.7015
	III	700.0769	0.8012	1.0913	1.8459
	IV	700.0216	0.6292	0.5703	1.3844
800	I	799.9150	1.2729	1.2455	2.3889
	II	802.5982	1.9962	28.4483	7.3299
	III	800.1744	1.0729	1.3213	2.2223
	IV	800.1440	0.7415	0.6173	1.5272
900	I	899.9358	1.1335	1.7688	3.1061
	II	897.1055	2.5599	49.0982	9.5669
	III	899.8045	1.0934	1.4579	2.3008
	IV	900.1746	0.7557	0.6268	1.5474
1000	I	1001.4265	1.7588	2.6090	3.5080
	II	1004.3600	3.2652	85.2401	12.4979
	III	1000.3473	1.1769	2.5278	2.7668
	IV	999.8078	0.7561	0.6971	1.5910
1100	I	1101.5444	2.0545	4.1117	4.0822
	II	1105.0904	6.2052	132.0428	17.6962
	III	1101.3222	1.4774	2.1067	2.9288
	IV	1100.3967	0.8274	0.7367	1.6857

The complex objects with convex-concave surface are measured and reconstructed by this way and these results are shown in Fig. 11a-c. In Fig. 11c is the result of measurement. The right side of the statue is not be reconstructed because the light is blocked. The result can be a true reflection of the measured surface. The feasibility and effectiveness of the method can be proved.

CONCLUSION

Asymmetric combined cycle-encoding light 3D measurement technique was presented. It was combined intensity ratio with cyclic code for the absolute intensity ratio to divide projection angle. By studying the comparative experiment the defect, periodic dislocation and the error of a cyclic code, which exist in traditional symmetric combined cycle-encoding light, is solved by symmetric combined cycle-encoding light. And the speed and accuracy of 3D measurement are improved effectively. The measurement error is less than 1.7 mm in the range of 1000 mm.

ACKNOWLEDGMENT

This study was supported by the National Natural Science Foundation of China (60572030) and the Harbin Key Scientific and Technological project (2005AA1CG152).

REFERENCES

Davis, J., D. Nehab, R. Ramamoorthi and S. Rusinkiewicz, 2005. Spacetime stereo: A unifying framework for depth from triangulation. Proc. IEEE Trans. Pattern Anal. Machine Intell., 27: 296-302.

Dong, B., Z. You, X.Z. Liu and Y.P. Li, 2000. Study on 3-D profile measurement method combining structured spatial code and gray level projection. Opt. Tech., 26: 9-12.

Guan, C., X. Yu and W. Haibin, 2007. RGB color Gray code based structured-light 3D measurement technique. Chinese J. Scientific Instrument, 28: 663-666.

Gühring, J., 2001. Dense 3-D surface acquisition by structured light using off the shelf components. Proc. SPIE Int. Soc. Opt. Eng., 4309: 220-231.

Lee, S., J. Choi, D. Kim, B. Jung, J. Na and H. Kim, 2004. An active 3D robot camera for home environment. Proc. IEEE Sensors, 1: 477-480.

Li, H.Y., F.P. Da and Y. Jin, 2006. Study on spatial encoding technique in 3D measurement. Applied Opt., 27: 344-349.

Pan, W., Y. Zhao and X.Y. Ruan, 2003. Application of phase shifting method in projection grating measurement. Applied Opt., 24: 46-49.

Pan, W., Y. Zhao and X.Y. Ruan, 2004. A new method for getting high precision phase in structural light measurement. Acta Opt. Sinica, 24: 687-692.

Sang, X.Z., 2001. A method on 3-D shape measurement and its trend in development. J. Beijing Inst. Machinery, 2: 36-37.

Xiaoyang, Y., H. Wu and Y. Liping, 2007. 3D measurement technology based on structured light by combining Gray code with phase-shift. J. Scientific Instrument, 28: 2152-2157.

Yu, X.Y. and H.B. Wu, 2008. Structured-light-based 3D measurement technique using Gray code and line-shift fringe. Chinese J. Scientific Instrument, 29: 701-706.

Zhang, S., 2003. 3D surface data acquisition for class CSE612. Department of Mechanical Engineering, SUNY at Stony Brook, Oct. 16, 2003. http://www.cs.sunysb.edu/~mueller/teaching/cse616/3D_data_acquisition.pdf.